Preprints of the 21st IFAC World Congress (Virtual)
Berlin, Germany, July 12-17, 2020

An Artificial Potential Field-Based Lithium-ion Battery SOC Equilibrium Method in Electric Vehicles

Fu Jiang *, **Cheng Jin** **, **Hongtao Liao** **, **Heng Li** *, **Yue Wu** **, **Yongjie Liu** **, **Jun Peng** *, **Zhiwu Huang** **

* *School of Computer Science and Engineering, Central South University, Changsha, 410083 China.*
** *School of Automation, Central South University, Changsha, 410083 China(Corresponding Author Email: liheng@csu.edu.cn).*

Abstract: A novel cell equilibrium algorithm which is used for battery state of charge equilibrium of battery pack is proposed in this paper. Cell equilibrium algorithm is a key technology for lithium-ion battery pack in the energy storage systems. In order to eliminate the imbalance of battery state of charge, it's generally controlled by adjusting the charging current. The artificial potential field can construct a virtual force function, which provides the mapping between state of charge deviation and charging current. Therefore, an artificial potential field-based equilibrium method to balance battery state of charge was proposed in this paper. By reasonably distributing the charging current of the battery, the equilibrium of the battery state of charge can be achieved. A laboratory testbed has been built to verify the effectiveness of the proposed method compared with conventional method. Experiment results analyzed the energy consumption and the convergence speed of state of charge deviation under artificial potential field control with different parameters.

Keywords: Li-ion battery, state-of-charge, equilibrium, artificial potential field, energy consumption

1. INTRODUCTION

Lithium-ion batteries are widely concerned for their advantages of small size, large capacity, light weight and high safety (Zhang, 2017).These advantages make it an important energy storage device in the 21st century. Meanwhile, It has laid an important foundation for the popularization of electric vehicles.

Generally, the energy storage capacity and higher voltage requirement can be achieved by connecting multiple batteries in series as a stack due to the voltage limit of a single battery. However, each battery has individual differences in an energy storage system, such as capacitance, internal resistance, self-discharge rate, and environmental condition. Overvoltage and undervoltage of lithium-ion batteries will seriously affect the health and safety of the systems (Isaacson et al., 1997) . If overvoltage occurs, production of CO_2, C_2H_4, and other gases will increase the internal temperature and pressure causing severe battery damage or an explosion(Affanni et al., 2005). If undervoltage occurs, internal reactions cause the cell to lose a large part of its capacity. Thus, equilibrium methods are particularly important to eliminate such an imbalance.

At present, the balance circuit of energy storage system is usually divided into two types: dissipative circuit and non-dissipative circuit(Li et al., 2017; Agrawal et al., 2016; Heng et al., 2018). A dissipative circuit is one in which excess energy is dissipated through passive components such as resistors. Non-dissipative circuits store excess energy in active components such as inductors or capacitors. When the battery voltage is too high, the active element either absorbs excess energy and stores or transfers it to a lower one. Although non-dissipative circuit has good energy efficiency, the disadvantages are its circuit complexity, control difficulty, bulky size. The dissipative balancing circuits are favored in low-power applications where the system size and cost budgets are limited, though the efficiency is relatively low.

In industrial applications, dissipative circuit and non-dissipative circuit have their own application. The differences between batteries still affect the equilibrium effect. Therefore, the equilibrium strategies are proposed to optimize the equilibrium effect. In general, equilibrium strategy can be classified into voltage equilibrium method and charge equilibrium method (Einhorn et al., 2010, 2011). Voltage equilibrium method is to equalize the voltages on every single cell after charging or discharging. Whereas, each battery exists the drawbacks of unequal internal resistances, battery voltage is unequal even though the battery capacity is equilibrium. Charge equilibrium method is a equilibrium scheme based on capacity of the individual cell. Both for charging and discharging an improvement of performance is gained when using the state of charge(SOC) and the capacity of the cells as information.

⋆ This work is supported by the National Natural Science Foundation of China (Grant Nos. 61672537 and 61803394). Corresponding Author: Heng Li, Email: liheng@csu.edu.cn

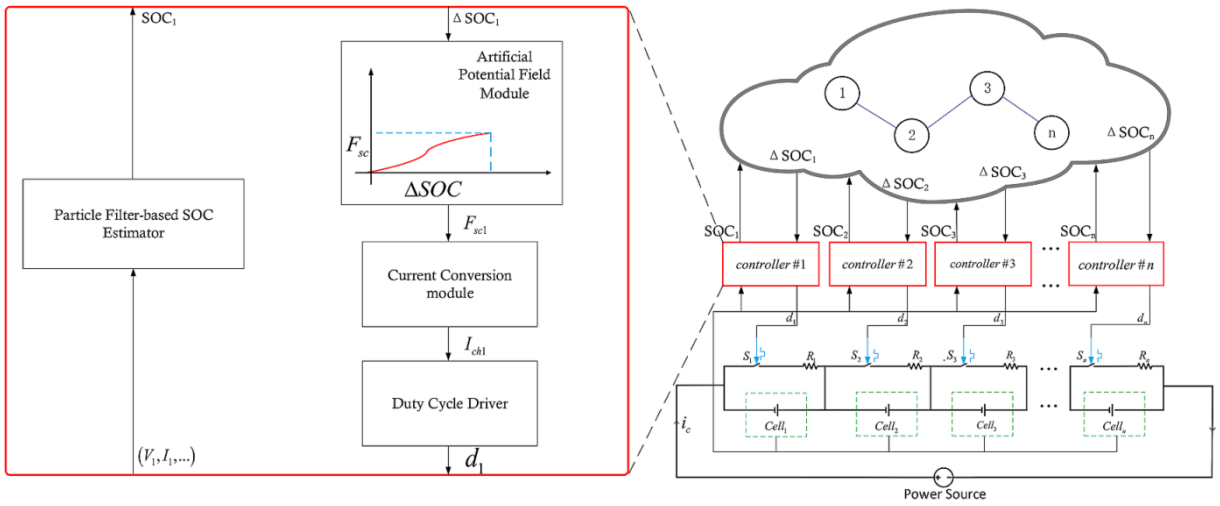

Fig. 1. The proposed cooperative cell equilibrium method for the switched resistor circuit.

In the equilibrium process, only a single battery is allowed to charge with simultaneous charging multi-cells being not allowable. In addition, the previous method aimed at the battery SOC to control. This control method is relatively complex and control systems are difficult to design(Aizpuru et al., 2013; Daowd et al., 2011; Vitols, 2014).

To address this challenge, a cell equilibrium control method for SOC deviation is designed in this paper. Artificial potential field is introduced to construct the mapping relationship between charge state deviation and charge current. This control method can accelerate the convergence of SOC deviation by controlling charging current. This SOC deviation-based mapping makes the control method simple and easy to implement. The effectiveness of the proposed method is verified compared with conventional method(Daowd et al., 2011). The energy consumption and the convergence speed of SOC deviation under different artificial potential field control parameters are analyzed.

The remainder of this paper is organized as follows. Section II introduces system schematic and artificial potential field. Section III gives the SOC estimation using particle filter. Section IV proposed the artificial potential field-based control strategy. Section V presents experimental results to demonstrate the good performance of the new control approach. We conclude the paper in Section VI.

2. SYSTEM SCHEMATIC AND ARTIFICIAL POTENTIAL FIELD

This section first introduces the schematic of the system, then the artificial potential field is given. It's the purpose to understand the system structure and control strategy.

2.1 System Schematic

We considered each cell as a single agent. The distributed control strategy is adopted to control the multi-agent system. This distributed control strategy greatly enhances the flexibility and reliability of the system(Caldon et al., 2014).

The schematic of the proposed cooperative cell equilibrium method is illustrated in Fig. 1. There are three layer in this system. The physical layer is the switched resistor circuit, where each cell is connected in parallel with a resistor via a switch. The control layer include the n controllers, which can collect the information of the physical layer and send control signal. The cyber layer describe the communication topology of each cells.

The process of the system schematic is as follows: (a) The information of each cell in switched resistor circuit was collected by the controller; (b) A SOC estimation algorithm calculated the SOC of each battery according to the collected information; (c) The SOC of every battery was shared with neighbor nodes through the communication module and got the deviation from the neighbor node; (d) the appropriate charging current was obtained according to the artificial potential field-based control strategy proposed in the paper; (e) The shunt switch adjusted the expected charging current according to the control signal given by the controller.

2.2 Artificial Potential Field

Artificial potential field is first proposed to be used for multi-agent obstacle avoidance (Khatib, 1986) and is widely used in multi-agent formation control (Olfati-Saber and R., 2006). In the allocation of hybrid energy storage vehicles, a virtual force field is established to generate a coupling relationship between several agents and form a stable formation among agents.

The artificial potential field-based real-time cell equilibrium strategy in this work should be capable of determining the charging current adaptively on the premise of ensuring SOC of battery limitations. Meanwhile, this strategy can accelerate the SOC convergence speed of lithium-ion battery.

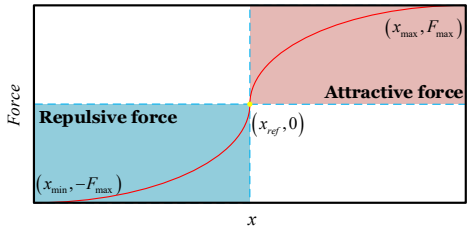

Fig. 2. The force of potential field.

The force function between any two agents is presented in Fig. 2(Wu et al., 2020), also called action function in this artificial potential field. When the distance between any two agents equals to the reference value, there is no force between them, i.e., the potential energy is zero. When two agents get close, there is a large repulsive force. When they are far away from each other, there is a large attractive force. This large attractive force or repulsive force, i.e., high potential energy, ensure the distance between them converges to the reference value quickly.

In the charging process, when ΔSOC is large, the force function will generate a strong gravitation forcing ΔSOC to the equilibrium point. When $\Delta SOC \to 0$, this gravitation will gradually weaken and eventually disappear.

3. SOC ESTIMATION USING PARTICLE FILTER

This section firstly introduced the RC first-order dynamic circuit, then the algorithm of particle filter is utilized to do SOC estimation based on the proposed nonlinear model. It's the purpose to obtain more accurate SOC of battery.

3.1 The Discrete Battery Model

The equivalent circuit model for Li-ion battery is a combination of voltage source, resistors and capacitors.The RC ladder characterizes the battery dynamics . Considering the accuracy and complexity of the model, we use the RC first-order dynamic circuit to describe the battery (Hu et al., 2012). The proposed battery circuit model is show in Fig. 3.

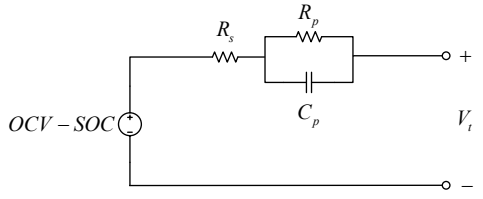

Fig. 3. The first order battery circuit model.

The state-space model is obtained based on the circuit in Fig. 3. Take the voltage across the RC ladder as U_p . Define the state variables as U_p and SOC. According to the circuit model, the state-space model is described by

$$\begin{bmatrix} dSOC/dt \\ dU_p/dt \end{bmatrix} = \begin{bmatrix} 0 & 0 \\ 0 & -\dfrac{1}{R_pC_p} \end{bmatrix} \begin{bmatrix} SOC \\ U_P \end{bmatrix} + \begin{bmatrix} -\dfrac{1}{C_n} \\ -\dfrac{1}{C_p} \end{bmatrix} I, \quad (1)$$

$$V_t = OCV\left(SOC\right) - U_p - R_sI, \quad (2)$$

where R_s represents the series resistance, R_p and C_p are the resistance and capacitance of the RC ladder.In this equation, the OCV-SOC table is expressed as an open circuit voltage (OCV) function.

Ah measurement method is the most commonly used SOC estimation method. If charge/discharge initial state is $SOC\left(t_0\right)$, then the $SOC\left(t\right)$ in the current state is

$$SOC\left(t\right) = SOC\left(t_0\right) + \int_0^t \frac{I\left(\tau\right)}{C_n} d\tau. \quad (3)$$

To obtain the discrete model, the discrete form for (3) is

$$SOC\left(k+1\right) = SOC\left(k\right) + \frac{\Delta t}{C_n} I\left(k\right), \quad (4)$$

where Δt is the sampling interval, k is the sampling step. The other state variable U_p is represented by the sum of RC circuits discrete-time zero-state response $R_p\left(1 - e^{-\frac{\Delta t}{R_pC_p}}\right) I\left(k\right)$ and discrete-time zero-input response $e^{-\frac{\Delta t}{R_pC_p}} U_p\left(k\right)$ approximately. Therefore, the discrete form of formula (1) and formula (2) is

$$\begin{bmatrix} SOC\left(k+1\right) \\ U_p\left(k+1\right) \end{bmatrix} = \begin{bmatrix} 1 & 0 \\ 0 & e^{-\frac{\Delta t}{R_p(SOC)C_p(SOC)}} \end{bmatrix} \begin{bmatrix} SOC\left(k\right) \\ U_p\left(k\right) \end{bmatrix} + \begin{bmatrix} -\dfrac{\Delta t}{C_n} \\ R_p\left(SOC\right)\left(1 - e^{-\frac{\Delta t}{R_p(SOC)C_p(SOC)}}\right) \end{bmatrix} I\left(k\right), \quad (5)$$

$$V_t\left(k\right) = OCV\left(SOC\left(k\right)\right) - U_p\left(k\right) - R_sI\left(k\right), \quad (6)$$

where R_p and C_p are functions of SOC. Then, the state vector is defined by

$$x_k = \left[\, SOC\left(k\right)\ U_p\left(k\right) \,\right]^T. \quad (7)$$

3.2 Particle Filter

In general, a nonlinear system is described by

$$x_k = f\left(x_{k-1}, u_{k-1}, w_{k-1}\right) \quad (8)$$

$$y_k = h\left(x_k, u_k, v_k\right), \quad (9)$$

where w_k and v_k are independent white noise with known probability distribution function (PDF). The system states are Markovian, i.e.,

$$P\left(x_k \,|x_{k-1}, x_{k-2}, \cdots, x_0\right) = P\left(x_k \,|x_{k-1}\right). \quad (10)$$

Then particle filter can be utilized to do state estimation for the system. Particle filter is a Monte Carlo method for implementing a recursive Bayesian filter. The posterior state is approximated by a set of weighted particles.The particle filter algorithm is described as follows:

Firstly, determine the number of particles M according to the systems form and computation cost. So, the initial particles are generated by

$$x_0^i = \hat{x}_0 + N\left(0, \sigma_0^2\right). \quad (11)$$

Secondly, for $i = 1, 2, \cdots, M$ particles, propagate the state particles $x_{k-1}^i \, (i = 1, 2, \cdots, M)$ to the next step by the system process equation,

$$x_k^i = f\left(x_{k-1}^i, u_{k-1}\right) + N\left(0, \sigma_{k-1}^2\right). \tag{12}$$

Thirdly, update and normalize the important weights for each particle. Calculate the ith particles likelihood and normalize the likelihood q_i of each particle as

$$q_i = \exp\left(-\frac{1}{2\sqrt{R}}\left(y_k - h\left(x_k^i, u_k\right)\right)^2\right) / \sqrt{2\pi R}, \tag{13}$$

$$\omega_k^i = \frac{q_i}{\sum_{j=1}^{M} q_j}. \tag{14}$$

Fourthly, a new particle set $\{\bar{x}_k^i\}_{i=1}^M$ is obtained by re-sampling to eliminate particles with small weights and to concentrate on particles with large weights.

Lastly, Calculate the mean of the re-sampled particles to obtain particle filters estimation result $\hat{x}_k$,

$$\hat{x}_k = \frac{1}{M} \sum_{i=1}^{M} \bar{x}_k^i. \tag{15}$$

4. THE ARTIFICIAL POTENTIAL FIELD-BASED CONTROL STRATEGY

A control strategy based on artificial potential field is introduced in this section. First, the artificial potential field calculates the virtual attractive force according to the SOC of the batteries, then the mapping relationship between the virtual force and the duty cycle of switch was established to adjust the charging/discharging current of each batteries.

4.1 Establishment of the artificial potential field

In this paper, We want the SOC of each cell to be consensus, i.e., ΔSOC=0. We considered the method of mutual attraction of each cell through a virtual force to achieve consensus. For example, there are three cells. When $\Delta SOC \geq 0$ between Cell A and Cell B, this virtual force makes the cells close to a certain median value. Meanwhile Cell B and Cell C also reach consensus in the same way. Eventually, all the cells will reach consensus.

We establish artificial potential field function to construct the relation between virtual force and SOC. First, according to the estimated SOC, we get the deviation between neighbor nodes

$$x = SOC_i - SOC_{i+1} \, (i = 1, 2, \cdots, m). \tag{16}$$

Then virtual SoC attractive forces can be defined as follows

$$F_{\text{sc}} = \arctan\left(\alpha x\right). \tag{17}$$

Eq (17) are depicted in Fig. 4(α=20). It is worth noticing that under this coordinate setting, the force $F_{\text{sc}} \geq 0$ when $\Delta SOC \geq 0$. Therefore, a positive force is provided to pull cell with higher SOC. Whereas a negative force is provided to push cell with lower SOC.

The related artificial potential energy function is defined as

$$U\left(x\right) = \int_{-1}^{1} \left|F_{\text{sc}}\left(x\right)\right| dx, \tag{18}$$

which are plotted in Fig. 5. It is clearly shown that the lowest potential energy point is $\Delta SOC = 0$. When the battery systems are imbalance ($\Delta SOC \neq 0$), a larger potential energy is provided so that SOC converges to zero.

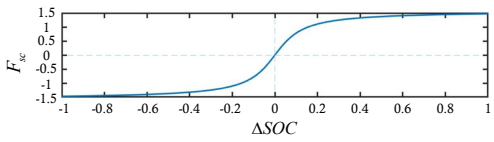

Fig. 4. Virtual attractive force $Fsc - SoC$ diagram

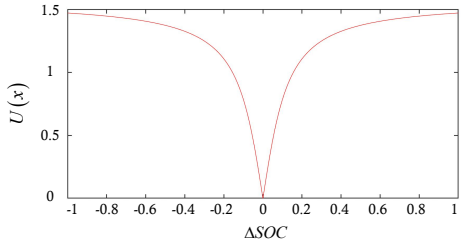

Fig. 5. Virtual potential energy $U(x) - SoC$ diagram.

4.2 Determination of charging/discharging current

An actual quantity that maps the virtual attractive force is needed during charging/discharging process. The appropriate charging/discharging current is selected to eliminate imbalance.

We take charging process as an example to analyze the relationship between virtual force and current. The normal charging current of lithium ion battery is about $0.2C \sim 1C$. We need to determine the appropriate charging current based on the virtual force

$$I_{ch} = \left[\frac{0.8\left(F_{\text{sc}} + 1.5\right)}{3} + 0.2\right] C, \tag{19}$$

where the constants are to limit I_{ch} in $[0.2C, C]$. In charging mode, $I_{ch} = 1C$ when ΔSOC is maximum, i.e., the cell is charging with the maximum safe current; $I_{ch} = 0.2C$ when ΔSOC is minimum. For both modes, when there is no force, $I_{ch} = 0.6C$.

5. EXPERIMENTAL VERIFICATION

In this section, we provide experiment results to illustrate the effectiveness of the proposed charging strategy.

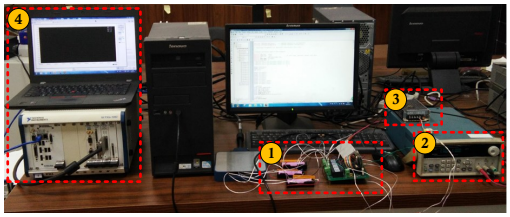

Fig. 6. Experiment hardware setup: (1) control board, three batteries and three resistors, (2) CC-CV power source, (3) DC 24V power source, (4) PXI platform.

5.1 Parameter Setting

The battery model number selected is ICR18650, the rated voltage is 3.7V and the capacity is 2200mAh. The initial SOC of three cells are different, and they are given as $SOC_1(0) = 0.6$, $SOC_2(0) = 0.55$, and $SOC_3(0) = 0.5$. The target SOC of each cell is 0.9. And 0.5Ω is chosen as the switched resistor in this experiment.

5.2 Platform Introduction

The hardware setup of the CC-CV cell equilibrium charging system is shown in Fig. 6. The experiment setup mainly includes four parts: (1) a control board, three batteries and three equilibrium resistors and color is yellow; (2) a DC 24 V power source; (3) a constant-current and constant-voltage power source; (4) a PXI platform. The CC-CV power source provides the charging current for the cells in this system, and the 24V DC power provides the operating voltage for the control board. The PXI platform collects the voltage of each cell and displays the waveforms on the NI-veristand in the hosting computer.

The main role of the control board is to adjust the switch to control the charging current. The function of the control board can be divide into voltage measurement module, control module, communication module, and CAN module. For the measurement accuracy is important, we choose three high-precision voltage sampling sensors to measure the terminal voltage of every batteries. The control algorithm will calculate the SOC based on the measured data. The algorithm is realized by the TMS3202808 microprocessor.

5.3 Verification Results

We compared the proposed control system which has the different artificial potential field parameters and collected their voltage waveforms and SOC waveforms. The no artificial potential field(α=0) control method is the conventional control method.(Daowd et al., 2011). The voltage waveform collected is shown in fig. 7. Fig. 7 (a), (b), (c) respectively represents the battery voltage curve under different parameters. As can be seen from fig. 7(a), the three batteries started charging at the same time. When the voltage limit is reached, the battery stopped charging. In fig. 7(b), the voltage of Cell3 started to rise first, then the voltages of Cell2 and Cell3 started to rise slowly. The voltage of the three batteries started to rise synchronously and eventually stopped charging when the voltage reaches its maximum when they are the equilibrium. In fig. 7(c), the three batteries also rose in equilibrium. Due to the different of artificial potential field parameters, the voltage rise speed of the three batteries before equilibrium was significantly different from that in fig. 7(b).

Fig. 8 visually shows the differences in the control methods of the three different parameters. As shown in fig. 8(a), SOC of the three batteries rose at the same rate. When the SOC reaches the upper limit, the SOC of the three batteries will be the equilibrium. In fig. 8(b), due to the moderate selection of parameters, the SOC of the three batteries reached the same level at 2231s. Compared with the cooperative control strategy without artificial potential field, The SOC equilibrium time was greatly advanced. In fig. 8(c), we considered an extreme case where the parameter of the artificial potential field was set as large as possible. We found that the SOC of the three batteries was almost the equilibrium at 983s. The SOC equilibrium time of three batteries was advanced with the increase of parameters.

Table 1. Energy consumption of shunt resistor.

Parameter	Energy consumption($w \cdot h$)
α_1=0	4.77
α_2=20	3.08
α_3=2000	4.79

However, this control method which makes the parameters of artificial potential field as large as possible has some disadvantages. It can be clearly observed from fig. 8(c) that in the process of SOC becoming equilibrium, the excess energy is consumed on the shunt resistance. Table 1 shows the energy consumption of the artificial potential field control method under three different parameters. We can see that when the parameters are too large, the system energy consumption is also large. From the experimental results, we can infer the relationship between the energy consumption of the system and the parameters into a concave function.

6. CONCLUSION

Charging equilibrium circuits are important for battery and developed to improve the reliability, property and lifetime. Different control strategies and their effectiveness have to be evaluated actually. The artificial potential field-based equilibrium algorithm for battery pack system was proposed in this paper. Firstly, a particle filter method is proposed to estimate SOC of lithium-ion battery. Then, the artificial potential field model is established to control SOC of lithium battery adaptively, so that the whole system can reach equilibrium quickly. The concept of artificial potential field is first referenced in the field of battery balance management system. Experimental results are provided to analyze the effectiveness of the design and the energy consumption of the system.

ACKNOWLEDGEMENTS

This work is supported by the National Natural Science Foundation of China (Grant Nos. 61672537 and 61803394).

REFERENCES

Affanni, A., Bellini, A., Franceschini, G., Guglielmi, P., and Tassoni, C. (2005). Battery choice and management for new-generation electric vehicles. *IEEE Transactions on Industrial Electronics*, 52(5).

Agrawal, B., Adam, M., Vadala, B., Koke, H., and Emadi, A. (2016). Non-dissipative battery cell balancing using half-bridge switching circuit. In *2016 IEEE Transportation Electrification Conference and Expo (ITEC)*.

Aizpuru, I., Iraola, U., Canales, J.M., Echeverria, M., and Gil, I. (2013). Passive balancing design for li-ion battery packs based on single cell experimental tests for a cccv charging mode. 93–98.

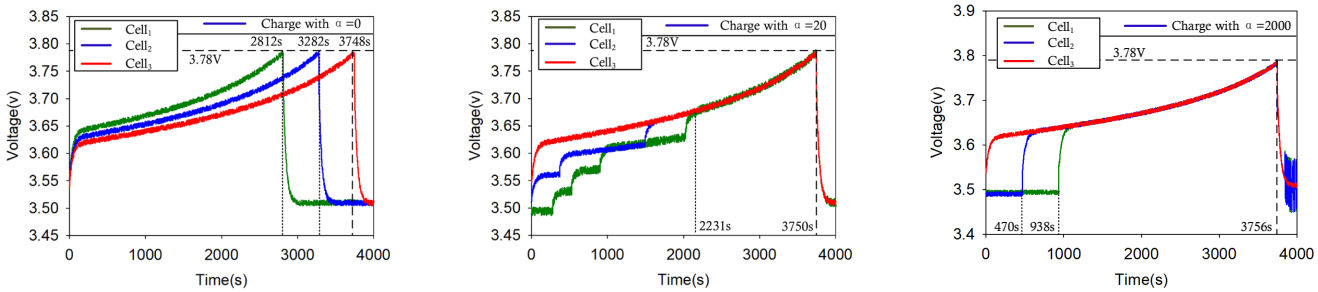

(a) The voltage of cells with no artificial potential field(conventional) control method.

(b) The voltage of cells with α=20 artificial potential field control method.

(c) The voltage of cells with α=2000 artificial potential field control method.

Fig. 7. The voltage curves of the different parameter artificial potential field control control method.

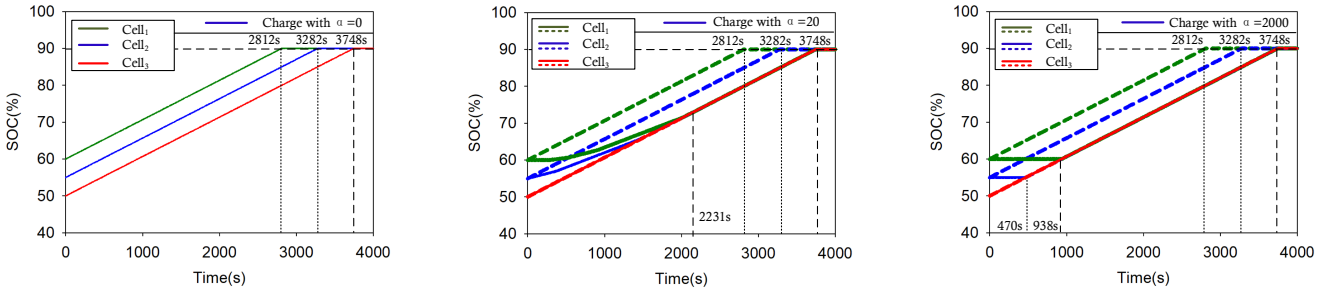

(a) The SOC of cells with no artificial potential field(conventional) control method.

(b) The SOC of cells with α=20 artificial potential field control method.

(c) The SOC of cells with α=2000 artificial potential field control method.

Fig. 8. The SOC curves of the different parameter artificial potential field control control method.

Caldon, R., Coppo, M., and Turri, R. (2014). Distributed voltage control strategy for lv networks with inverter-interfaced generators. 107(2), 85–92.

Daowd, M., Omar, N., Van den Bossche, P., and Van Mierlo, J. (2011). A review of passive and active battery balancing based on matlab/simulink. *Journal of International Review of Electrical Engineering (IREE)*, 6, 2974–2989.

Einhorn, M., Roessler, W., and Fleig, J. (2011). Improved performance of serially connected li-ion batteries with active cell balancing in electric vehicles. *IEEE Transactions on Vehicular Technology*, 60(6), 2448–2457.

Einhorn, M., Conte, F.V., and Fleig, J. (2010). Improving of active cell balancing by equalizing the cell energy instead of the cell voltage. *World Electric Vehicle Journal*, 4(2), 400–404.

Heng, L., Jun, P., Yanhui, Z., Jianping, H., Zhiwu, H., Liang, H., and Jianping, P. (2018). Soh-aware charging of supercapacitors with energy efficiency maximization. *IEEE Transactions on Energy Conversion*, 1–1.

Hu, X., Li, S., and Peng, H. (2012). A comparative study of equivalent circuit models for li-ion batteries. *Journal of Power Sources*, 198, 359–367.

Isaacson, M.J., Hollandsworth, R.P., Giampaoli, P.J., Linkowsky, F.A., Salim, A., and Teofilo, V.L. (1997). Advanced lithium ion battery charger. In *Battery Conference on Applications & Advances*.

Khatib, O. (1986). Real-time obstacle avoidance system for manipulators and mobile robots. 5(1), 90–98.

Li, L., Huang, Z., Li, H., and Peng, J. (2017). A rapid cell voltage balancing scheme for supercapacitor based energy storage systems for urban rail vehicles. *Electric Power Systems Research*, 142, 329–340.

Olfati-Saber and R. (2006). Flocking for multi-agent dynamic systems: algorithms and theory. *IEEE Transactions on Automatic Control*, 51(3), 401–420.

Vitols, K. (2014). Design of an embedded battery management system with passive balancing. In *2014 6th European Embedded Design in Education and Research Conference (EDERC)*.

Wu, Y., Huang, Z., Liao, H., Chen, B., Zhang, X., Zhou, Y., Liu, Y., Li, H., and Peng, J. (2020). Adaptive power allocation using artificial potential field with compensator for hybrid energy storage systems in electric vehicles. *Applied Energy*, 257(2), 113983.

Zhang, S. (2017). Chemomechanical modeling of lithiation-induced failure in high-volume-change electrode materials for lithium ion batteries. 3(1).